Journal of Communication Engineering (JCE)

P- ISSN: 2322-4088 Vol. 12, No. 1, Jan.-Jun. 2023 E- ISSN: 2322-3936

Statistical Analysis of Connectivity Enhancement for Cell-Edge Users in MIMO-Enabled Wireless Cellular Networks Using Cooperative Non-Orthogonal Multiple Access (CNOMA) with Power Allocation

Asma Bagheri* **[Corresponding Author]** Department of Electrical Engineering; Esfarayen University of Technology; Esfarayen, North Khorasan, Iran;
Email: bagheri.asma84@yahoo.com

Mohammad Amin Karimi Department of Electrical Engineering; Esfarayen University of Technology; Esfarayen, North Khorasan, Iran;
Email: makarimi.ee@gmail.com

Received: *26 Feb. 2023* ***Revised:*** *29 Apr. 2023* ***Accepted:*** *06 Jun. 2023*

Abstract: This paper investigates the integration of Cooperative Non-Orthogonal Multiple Access (CNOMA) with Multiple-Input Multiple-Output (MIMO) technology to enhance connectivity for cell-edge users in wireless cellular networks. In the proposed framework, intra-cell users act as relays to forward data to cell-edge users, improving signal reception through selection and spatial diversity provided by MIMO antennas. Connectivity analysis is essential to evaluate Quality of Service (QoS) and overall network performance, but it is complicated by channel fading, MIMO channel correlation, and the influence of successive interference cancellation (SIC) in relay users. To address these challenges, we develop a closed-form expression for the connectivity probability of cell-edge users in CNOMA-based MIMO networks. The model assumes Rayleigh fading channels, exponential channel gain distributions, and distinct power allocation for each sub-channel. By analytically modeling the Signal-to-Interference-plus-Noise Ratio (SINR) and applying a Gamma approximation, we derive a closed-form solution under imperfect SIC conditions, incorporating the probability of SIC success in relay users. Simulation results validate the analytical findings and provide insights into performance enhancement, offering a practical framework for designing robust CNOMA-MIMO systems for improved cell-edge connectivity.

Citation: Asma Bagheri and Mohammad Amin Karimi, "Statistical Analysis of Connectivity Enhancement for Cell-Edge Users in MIMO-Enabled Wireless Cellular Networks Using Cooperative Non-Orthogonal Multiple Access (CNOMA) with Power Allocation," *Journal of Communication Engineering*, vol. 12, no. 1, pp. 91-108, Jan.-Jun. 2023.
http://dx.doi.org/10.22070/jce.2026.19475.1273

Index Terms: Cooperative-NOMA; Connectivity; Imperfect SIC; MIMO Systems; Rayleigh Fading.

I. INTRODUCTION

NOMA (non-orthogonal multiple access) presents a promising technique for beyond fifth-generation (B5G) networks, offering low latency, high reliability, better spectral efficiency, and enhanced connectivity performance compared to OMA [1]. The significance of connectivity analysis in wireless cellular networks lies in its role in understanding user connections and overall network performance. This analysis allows for the modeling and evaluation of connectivity probability, crucial for determining communication success between users and base station (BS), Quality of Service (QoS), and overall network performance [2].

Cooperative NOMA (CNOMA) has the potential to improve the connectivity of cell-edge users in cellular networks. Unlike conventional NOMA, where more power is allocated to the cell-edge user than the near user, CNOMA proposes further enhancement of the cell-edge user's rate [3]. In CNOMA, the near user can serve as a relay, retransmitting the cell-edge user's signal and thereby enhancing the signal strength at the cell-edge through selection diversity [4], [5]. Consequently, CNOMA-based networks enhance network scalability with fair resource allocation [1], with applications extending to various domains including 5G and B5G networks, IoT, smart cities, and mission-critical communication systems. As such, the significance of CNOMA-based wireless cellular network analyses and its practical applications are pivotal for shaping the future of wireless communication technologies and enabling a wide range of transformative applications and services.

MIMO Cooperative Non-Orthogonal Multiple Access (MIMO-Cooperative NOMA) combines the benefits of MIMO (Multiple-Input Multiple-Output) and Cooperative NOMA techniques to enhance wireless communication performance, particularly in scenarios with varying channel conditions and distances to users. It leverages the advantages of both technologies to improve spectral efficiency, reliability, and coverage [6], [7].

Given the random behavior of wireless channels, such as fading effects, analyzing and understanding the statistical features of connectivity, especially for cell-edge users in CNOMA-based networks, becomes essential for devising efficient resource allocation strategies, relay selection mechanisms, and interference management techniques [8]. Investigating the impact of user collaboration on connectivity paves the way for the development of advanced wireless

networks capable of supporting diverse applications and a massive number of connected devices. With the growing demand for high data rates and reliable connectivity, the analysis of connectivity in CNOMA-based wireless cellular networks emerges as a crucial point for advancing the performance and capabilities of next-generation wireless communication systems.

In this paper, we present a statistical analysis of the cooperative non-orthogonal multiple access (CNOMA) technique to enhance connectivity for cell-edge users in wireless cellular networks. Our study focuses on exploring the use of intra-cell users as relays within to tackle connectivity challenges of cell-edge users with specific consideration given to the effects of channel fading and successive interference cancellation (SIC) on relay users. Our key contribution involves providing a comprehensive evaluation of how CNOMA impacts connectivity and service quality for users at the cell edge. To this end, we provide a closed-form expression for the connectivity probability of a cell-edge user in a CNOMA-based cellular network, assuming Rayleigh fading channels and the probability of successive interference cancellation (SIC) in relay users, which shows the impact of user collaboration on connectivity. Furthermore, our analysis also covers other scenarios such as conventional NOMA and orthogonal multiple access (OMA) techniques. Finally, the simulations are conducted to evaluate the derived expression for the connectivity. Through detailed simulation results and statistical analysis, we explore the potential advantages and obstacles associated with deploying CNOMA, conventional NOMA, and OMA within wireless cellular networks. Ultimately, our research seeks to contribute to the enhancement of cellular network performance and address the increasing need for improved connectivity in wireless communications.

The rest of this paper is organized as follows. In section 2, we review previous related works. Section 3, describes the system model of the CNOMA-based wireless cellular network. Section 4 explains the main results. In Section 5, numerical results are presented to evaluate the derived closed-form expression for connectivity of the cell-edge user. In Section 6, we conclude the paper.

II. RELATED WORKS

In wireless cellular networks, connectivity analysis is vital for ensuring successful communication especially for the cell-edge users. Numerous studies have focused on modeling and analyzing connectivity, providing valuable insights into enhancing network performance. Notably, research in this domain explores how cooperative strategies, such as user cooperation, amplify-and-forward relaying, and decode-and-forward relaying, can augment the connectivity and overall performance of wireless cellular networks. The following presents a discussion of some recent relevant works on NOMA and CNOMA-based wireless cellular networks.

A comprehensive review by [9] encompasses various investigations on (Simultaneous Wireless Information and Power Transfer) SWIPT-aided CNOMA networks, offering system design guidelines, performance analysis, and diverse communication protocols. Additionally, it provides an in-depth examination of studies based on relay type, number of relays, and communication protocol. Also, recent relevant works delve into improving outage probability and sum throughput in NOMA systems through cooperative relaying schemes, as proposed in [4]. These schemes leverage intra-cell users as relays to aid direct transmission to cell-edge users, incorporating an on/off mechanism based on known link quality. Furthermore, [10] investigates the performance of cell-edge users in a MISO-NOMA system and proposes three cooperative downlink transmission schemes to enhance performance.

Expanding the scope, [11] analyzes a cooperative downlink multi-user (MU) multiple-input single-output (MISO) NOMA IoT network, aiming to enhance the performance of IoT devices with weak channel conditions by selecting a user with better reception as a relay node. The system model integrates SWIPT protocols for energy harvesting and transmission, while investigating power allocation coefficients and user selection methods to improve performance. Additionally, [2] examines the performance of NOMA-based full-duplex IoT relay systems with SWIPT over Nakagami-m fading channels. It derives closed-form expressions for system throughput, energy efficiency, and ergodic capacities. Another study, [12], examines two transmission scenarios for serving cell-edge users in cellular networks, utilizing a transmit antenna selection (TAS) policy to significantly enhance system performance in NOMA networks. Moreover, [13] introduces a D2D-relay communication model to elevate cell-edge user coverage quality, formulating a resource allocation problem and proposing an iterative power allocation algorithm. However, these studies do not specifically address the connectivity probability of cell-edge users.

Furthermore, [14] proposes a single-cell CNOMA system with energy harvesting full-duplex (FD) relaying to amplify the sum rate and energy efficiency in cellular networks, considering a downlink model with a BS, intra-cell users, and cell-edge users. This approach incorporates an FD decode and forward (DF) relay to enhance the performance of a cell-edge user, along with optimization problems for power allocation to maximize sum rate and energy efficiency. Furthermore, [15] investigates the performance of TSB-CNOMA (Two-Stage Beamforming Cooperative Non-Orthogonal Multiple Access) in wireless networks, analyzing the bit error probability (BEP) of TSB-CNOMA for different modulation pairs of users in various channel fading conditions. While addressing the performance analysis of TSB-CNOMA, this study does not specifically explore the connectivity of cell-edge users.

Through synthesizing and analyzing these diverse studies, this paper explores the broader

understanding and provides statistical analysis for connectivity within NOMA-based wireless cellular networks, particularly focusing on the significance of cooperative and its impact on the connectivity of cell-edge users.

Recent advances in cooperative NOMA and MIMO technologies have motivated a range of studies aimed at improving wireless system performance. In [16], the performance of MIMO-NOMA systems under imperfect SIC is evaluated through capacity and outage metrics but lacks cooperative mechanisms and vectorized power modeling. In [7], a more complex OAM-MIMO framework is adopted for 6G systems, emphasizing ergodic capacity enhancement via full-duplex relaying, yet it assumes Nakagami-m fading and does not address connectivity metrics. The work in [17] investigates power-ordered NOMA with massive MIMO and SC-FDE, but its scope is limited to single-carrier transmission and does not incorporate subchannel-specific SINR modeling. Reference [18] presents a comprehensive survey of cooperative PD-NOMA integrated with technologies such as RIS and ML but offers no analytical derivation or performance quantification. Studies in [19] and [20] respectively focus on outage optimization and power minimization through large-scale MIMO configurations and beamforming strategies, but they rely heavily on simulations and do not capture the probabilistic behavior of user connectivity.

In contrast, our work uniquely develops a statistical MIMO CNOMA-based framework that incorporates vectorized power allocation and subchannel-specific SINR expressions, and further derives closed-form Gamma-approximated expressions for the connectivity and outage probabilities of cell-edge users under Rayleigh fading. Importantly, none of the aforementioned studies address the core objective of our paper: the analytical derivation of closed-form statistical expressions for the connectivity probability of the cell-edge user in CNOMA-based MIMO systems.

While our previous work addressed a similar problem, it was restricted to a single-antenna (SISO) configuration and therefore could not capture the inherent benefits of MIMO systems [8]. In the prior analysis, neither vectorized power allocation nor matrix-based formulations were incorporated, which limited the analysis to overly simplified scenarios and prevented the exploitation of spatial diversity and flexible resource allocation. In contrast, the present work significantly broadens the scope by incorporating multiple antennas and explicitly leveraging spatial diversity gain, which ensures that even if some propagation paths suffer from deep fading, other independent paths can sustain the communication link. This markedly enhances both system reliability and overall performance. Beyond spatial diversity, the proposed framework is highly general and flexible, as the derived closed-form expressions seamlessly cover the entire spectrum of system configurations from the basic SISO case ($N = 1$), to small-scale MIMO ($N = 2$), and up

to large-scale and Massive MIMO deployments ($N >> 2$). This generality is particularly valuable for system designers, since it allows the evaluation of a wide variety of configurations within a unified analytical model, eliminating the need for separate case by case formulations.

Another major advancement of the present work is the introduction of vectorized power allocation, which provides additional degrees of freedom for optimizing performance. Unlike the SISO case, where each user could only be assigned a single power coefficient, the MIMO framework enables the distribution of power across multiple antennas or sub-channels. This flexibility allows for more sophisticated strategies, such as emphasizing stronger channels to boost throughput or balancing allocation across weaker ones to enhance fairness. The direct performance benefits of this capability are explicitly demonstrated in the numerical results.

Equally important, this extension brings the analysis closer to real-world scenarios, as modern wireless technologies from 5G and emerging 6G networks to Wi-Fi 6/6E and Wi-Fi 7 are fundamentally built around MIMO architectures, where heterogeneous and dynamic power allocation across multiple antennas is standard. Consequently, analyzing the generalized N-dimensional case is not merely a theoretical exercise but a practical necessity to ensure that the derived insights and performance characterizations are directly applicable to contemporary and future networks. To achieve this, the present study employs advanced probabilistic tools, such as the Gamma distribution approximation and weighted exponential sums, to accurately model the aggregate effect of multiple sub-channels. This methodological improvement enables the derivation of precise closed-form expressions for the connectivity probability, going far beyond the simplified exponential models used in previous SISO work. As a result, the current analysis not only provides a more realistic and general evaluation of system performance but also offers a deeper theoretical understanding of CNOMA systems in MIMO environments.

III. SYSTEM MODEL

This section describes the downlink model in a CNOMA-based cellular network with a base station (BS) and two mobile users (U1 and U2), where each node may be equipped with one or more antennas as shown in **Fig. 1** and the communication takes place over N parallel sub-channels (e.g., in OFDM systems or frequency-selective fading environments). In this system, during the first transmission phase, the BS sends signals to the users using the NOMA technique due direct links. Here, $a_{1i} < a_{2i}$, and x_1, x_2 denote the power allocation (PA) coefficients for each user over the i-th sub-channel and the corresponding user signals, respectively. Without loss of generality, it is assumed that $a_{1i} < a_{2i}$ for all sub-channels $i \in \{1,2, ..., N\}$. During the second phase, a threshold-based cooperative relaying scheme is assumed, in which the user with better aggregate channel

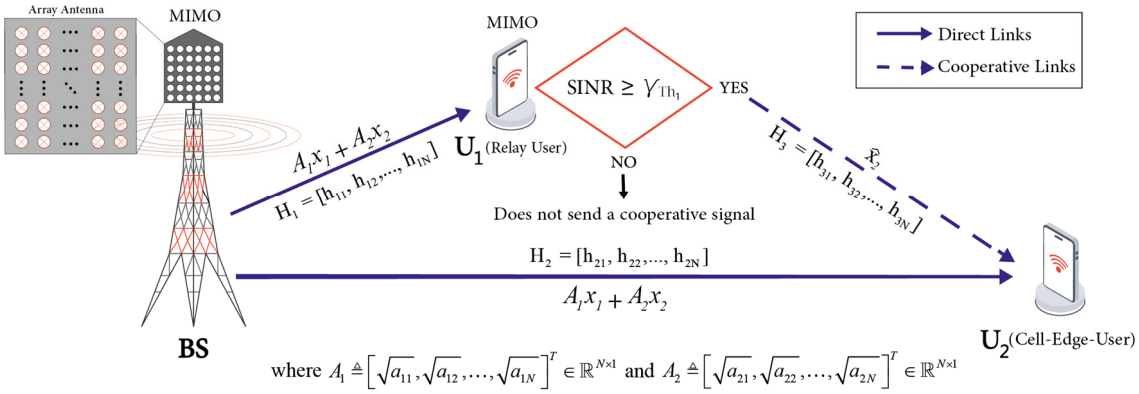

Fig. 1. MIMO-CNOMA System Model

conditions across all sub-channels (U1) forwards a cooperative signal (i.e., $\hat{x}_2$) to the cell-edge user (U2) with weaker channel conditions if and only if the overall signal-to-interference plus noise ratio (SINR) across all sub-channels at U1 is greater than a predetermined threshold value (i.e., γ_{Th1}). To do this, U1 considers its signal as noise and uses SIC to decode the cell-edge user's signal. In this scenario, U2 receives signals from both the BS and U1. It then uses the maximal-ratio combining (MRC) technique to achieve the maximum SINR.

We assume Rayleigh fading to model each wireless link across all sub-channels, with independent channel coefficients, denoted as h_{1i}, h_{2i}, and h_{3i} for the direct links between BS-U1, BS-U2, and the cooperative link between U1-U2 on the i-th sub-channel, respectively.

$$h_{ji} \sim \text{Rayleigh}\left(0, {\sigma_{ji}}^2\right) \quad , \quad j \in \{1,2,3\} \quad , \quad i \in \{1,2,\dots,N\} \tag{1}$$

Here, ${\sigma_{ji}}^2$ represents the variance of the channel, capturing the average power of the fading, while the Rayleigh distribution captures the small-scale multipath fading typical in wireless environments. This formulation ensures that the received signal power across sub-channels is statistically independent and accounts for the realistic variations of wireless links.

In Equation (1), the subscript i denotes the index of the MIMO sub-channel between each transmitter receiver pair, while the subscript j indicates the co rresponding link. Specifically, j = 1 refers to the link between the BS and U1, j = 2 corresponds to the link between the BS and U2, and j = 3 represents the cooperative (D2D)[1] link between U1 and U2.

In the first phase of communication, BS implements superposition coding (SC) and transmits the total signal of users; hence, the received signals by the users are given as follows:

$$y_j = \sqrt{P_T} H_j (A_1 x_1 + A_2 x_2) + n_j \tag{2}$$

where P_T and n_j denote the total transmission power at BS and the additive white Gaussian noise (AWGN, $CN(0, N_0)$) observed at link j where $j \in \{1,2,3\}$, respectively.

1 Device to Device

The channel associated with link j is modeled by the vector $H_j \triangleq [h_{j1}, h_{j2}, \dots, h_{jN}] \in \mathbb{C}^{1\times N}$, where each complex coefficient h_{ji} represents the channel gain between the i-th transmit antenna and the receiver corresponding to link j. The transmit beamforming (or power allocation) vectors corresponding to the information symbols x_1 and x_2 are defined as $A_1 \triangleq [\sqrt{a_{11}}, \sqrt{a_{12}}, \dots, \sqrt{a_{1N}}]^T \in \mathbb{R}^{N\times 1}$, $A_2 \triangleq [\sqrt{a_{21}}, \sqrt{a_{22}}, \dots, \sqrt{a_{2N}}]^T \in \mathbb{R}^{N\times 1}$, where a_{ki} denotes the power allocated to symbol $x_k \in \{x_1, x_2\}$ at the i-th transmit antenna. This structure enables flexible power distribution for each data stream across the N antennas. Expanding the received signal yields the following equivalent representation:

$$y_j = \sqrt{P_T} \cdot [h_{j1}, h_{j2}, \dots, h_{jN}] \cdot \left(\begin{bmatrix} \sqrt{a_{11}} \\ \sqrt{a_{12}} \\ \vdots \\ \sqrt{a_{1N}} \end{bmatrix} x_1 + \begin{bmatrix} \sqrt{a_{21}} \\ \sqrt{a_{22}} \\ \vdots \\ \sqrt{a_{2N}} \end{bmatrix} x_2 \right) + n_j = \sqrt{P_T} \sum_{i=1}^{N} h_{ji}\left(\sqrt{a_{1i}} x_1 + \sqrt{a_{2i}} x_2\right) + n_j \quad (3)$$

which clearly illustrates the aggregated contributions of all transmit antennas to the received signal over link j, taking into account both data streams and their respective beamforming vectors. Accordingly, in the first phase, considering vectorized power allocation and multiple sub-channels, the received SINR at each user is written as follows:

$$\gamma_1 = \frac{\gamma_0 \sum_{i=1}^{N} a_{1i}|h_{1i}|^2}{\gamma_0 \sum_{i=1}^{N} a_{2i}|h_{1i}|^2 + 1} \quad (4)$$

$$\gamma_2 = \frac{\gamma_0 \sum_{i=1}^{N} a_{2i}|h_{2i}|^2}{\gamma_0 \sum_{i=1}^{N} a_{1i}|h_{2i}|^2 + 1} \quad (5)$$

Where $\gamma_0 = \frac{P_T}{N_0}$ denotes the average SNR. Also, the received SINR at U1, corresponding to the detection of the signals intended for U2 across all sub-channels, when U1 considers its own signals as noise and interference, (denoted as γ_{12}) is given as:

$$\gamma_{12} = \frac{\gamma_0 \sum_{i=1}^{N} a_{2i}|h_{1i}|^2}{\gamma_0 \sum_{i=1}^{N} a_{1i}|h_{1i}|^2 + 1} \quad (6)$$

If the SINR at U1 is greater than the threshold value (i.e., $\gamma_{12} \geq \gamma_{Th1}$), at the second phase of communication, it forwards a vector of cooperative signals to U2. Hence, the received signal by U2, in the second phase, is given as:

$$y_3 = \begin{cases} \sum_{i=1}^{N} n_{3i} & ; \gamma_{12} < \gamma_{Th1} \\ \sum_{i=1}^{N} \sqrt{P_T} h_{3i} \hat{x}_{2i} + n_{3i} & ; \gamma_{12} \geq \gamma_{Th1} \end{cases} \quad (7)$$

Here, n_{3i} denotes the AWGN distributed as $CN(0, N_0)$. U2 implements a maximum-ratio combining (MRC) for the received signals in two phases, and the total received signal by U2 is given as:

$$y_{tot2} = \begin{cases} \sum_{i=1}^{N} \sqrt{P_T} h_{2i} \left(\sqrt{a_{1i}} x_{1i} + \sqrt{a_{2i}} x_{2i} \right) + n_i & ; \ \gamma_{12} < \gamma_{Th1} \\ \sum_{i=1}^{N} \sqrt{P_T} (h_{3i} \hat{x}_{2i} + h_{2i} \left(\sqrt{a_{1i}} x_{1i} + \sqrt{a_{2i}} x_{2i} \right)) + n_i & ; \ \gamma_{12} \geq \gamma_{Th1} \end{cases} \quad (8)$$

Accordingly, the total received SINR at U2 is written as:

$$\gamma_{tot2} = \begin{cases} \gamma_2 = \frac{\gamma_0 \sum_{i=1}^{N} a_{2i} |h_{2i}|^2}{\gamma_0 \sum_{i=1}^{N} a_{1i} |h_{2i}|^2 + 1} & ; \ \gamma_{12} < \gamma_{Th1} \\ \gamma_2 + \gamma_c = \frac{\gamma_0 (\sum_{i=1}^{N} a_{2i} |h_{2i}|^2 + \sum_{i=1}^{N} |h_{3i}|^2)}{\gamma_0 \sum_{i=1}^{N} a_{1i} |h_{2i}|^2 + 1} & ; \ \gamma_{12} \geq \gamma_{Th1} \end{cases} \quad (9)$$

In the next section, we analyze the connectivity and outage of the cell-edge user over the downlink in the described CNOMA-based cellular network. Since the connectivity and outage behavior of U1, i.e., the intra-cell user, remains the same as conventional NOMA, the connectivity and outage are derived for only the cell-edge user.

IV. MAIN RESULTS

The connectivity probability (CP) of a user is defined as the probability that the received SINR exceeds a required threshold for successfully detecting the intended message with an acceptable error rate. The primary objective of this paper is to analyze and evaluate the connectivity probability of the cell-edge user. Accordingly, we compute the CP of U2 as the probability that the received SINR at the user satisfies $\gamma_{tot2} \geq \gamma_{Th2}$, where γ_{Th2} denotes a threshold level related to the sensitivity of the user's receiver. It is noted that the channel fading coefficients and the decision to cooperate at U1 are assumed to be statistically independent. Therefore, the connectivity probability of U2 in the CNOMA-based cellular system can be formulated as shown in Equation (10).

$$CP_{MIMIO\_CNOMA} = P\{\gamma_{tot2} \geq \gamma_{Th2}\} = \quad (10)$$
$$P\{\gamma_{12} < \gamma_{Th1}\}.P\{\gamma_2 \geq \gamma_{Th2}\} + P\{\gamma_{12} \geq \gamma_{Th1}\}.P\{\gamma_2 + \gamma_c \geq \gamma_{Th2}\} = P_1 P_2 + \bar{P}_1 P_3 =$$
$$P\{\gamma_{12} < \gamma_{Th1}\}.P\left\{\frac{\gamma_0 \sum_{i=1}^{N} a_{2i} |h_{2i}|^2}{\gamma_0 \sum_{i=1}^{N} a_{1i} |h_{2i}|^2 + 1} \geq \gamma_{Th2}\right\} + P\{\gamma_{12} \geq \gamma_{Th1}\}.P\left\{\frac{\gamma_0 (\sum_{i=1}^{N} a_{2i} |h_{2i}|^2 + \sum_{i=1}^{N} |h_{3i}|^2)}{\gamma_0 \sum_{i=1}^{N} a_{1i} |h_{2i}|^2 + 1} \geq \gamma_{Th2}\right\}$$

First, the individual probabilities P_1, $\bar{P}_1$, P_2, and P_3 in Equation (10) are computed separately. The probability P_1 is calculated as shown in Equation (11),where $\beta_i \triangleq (a_{2i} - \gamma_{Th1} a_{1i})^2$ and $\rho_{Th1} \triangleq \frac{\gamma_{Th1}}{\gamma_0}$.

$$P_1 = P\{\gamma_{12} < \gamma_{Th1}\} = P\left\{\frac{\gamma_0 \sum_{i=1}^{N} a_{2i} |h_{1i}|^2}{\gamma_0 \sum_{i=1}^{N} a_{1i} |h_{1i}|^2 + 1} < \gamma_{Th1}\right\} = P\{\sum_{i=1}^{N} \beta_i |h_{1i}|^2 < \rho_{Th1}\} \quad (11)$$

In these expressions, $|h_{1i}|^2$, $|h_{2i}|^2$, and $|h_{3i}|^2$ respectively represent the vectorized channel power gains of the direct links between BS-U1, BS-U2, and the cooperative link between U1 and U2. Since the channel fading coefficients follow a Rayleigh distribution, the squared magnitudes

$|h_{1i}|^2$, $|h_{2i}|^2$, and $|h_{3i}|^2$ follow exponential distributions, as the square of a Rayleigh-distributed random variable yields an exponential distribution [21].

$$|h_{ji}|^2 \sim Exp(\lambda_{ji}) \ , \ i \in \{1,2,\dots,N\} \ , \ j \in \{1,2,3\} \tag{12}$$

It is also well-established that the ratio of a weighted sum of independent and identically distributed exponential random variables (with equal weights and identical parameters) can be effectively approximated by a Gamma distribution [22]. Specifically, in our model, the channel power gain for the *i-th* sub-channel, denoted by $|h_{1i}|^2$, follows an exponential distribution with parameter $|h_{1i}|^2 \sim Exp(\lambda_{1i})$. Based on this approximation, the probability P_1 is analytically evaluated in a closed-form expression, where $Z \triangleq \sum_{i=1}^{N} \beta_i |h_{1i}|^2 and\ Z \sim Gamma(k_Z, \theta_Z)$.

$$P_1 = P\{Z < \rho_{Th1}\} = F_Z(\rho_{Th1}) = \int_0^{\rho_{Th1}} f_Z(z)dz = \int_0^{\rho_{Th1}} \frac{1}{\Gamma(k_Z)\theta_Z^{k_Z}} z^{k_Z-1} e^{-\frac{z}{\theta_Z}} dz = \frac{\gamma(k_Z, \frac{\rho_{Th1}}{\theta_Z})}{\Gamma(k_Z)} \tag{13}$$

Hence, based on Equation (13), the complementary probability of P_1, denoted by $\bar{P}_1$, is given by [21]:

$$\bar{P}_1 = 1 - P_1 = 1 - P\{Z < \rho_{Th1}\} = P\{Z \geq \rho_{Th1}\} = 1 - \frac{\gamma\left(k_Z, \frac{\rho_{Th1}}{\theta_Z}\right)}{\Gamma(k_Z)} = \frac{\Gamma\left(k_Z, \frac{\rho_{Th1}}{\theta_Z}\right)}{\Gamma(k_Z)} \tag{14}$$

The probability P_2 is calculated as shown in Equation (15),

$$P_2 = P\{\gamma_2 \geq \gamma_{Th2}\} = P\left\{\frac{\gamma_0 \sum_{i=1}^{N} a_{2i}|h_{2i}|^2}{\gamma_0 \sum_{i=1}^{N} a_{1i}|h_{2i}|^2 + 1} \geq \gamma_{Th2}\right\} = P\left\{\sum_{i=1}^{N} \tau_i |h_{2i}|^2 \geq \rho_{Th2}\right\} \tag{15}$$

where $\tau_i \triangleq (a_{2i} - \gamma_{Th2} a_{1i})\ and\ \rho_{Th2} \triangleq \frac{\gamma_{Th2}}{\gamma_0}$. Similarly, the probability P_2 is also computed using a Gamma approximation, in accordance with relation (13), as follows:

$$P_2 = P\{W \geq \rho_{Th2}\} = F_W(\rho_{Th2}) = \int_{\rho_{Th2}}^{\infty} f_W(w)dw = \int_{\rho_{Th2}}^{\infty} \frac{1}{\Gamma(k_W)\theta_W^{k_W}} w^{k_W-1} e^{-\frac{w}{\theta_W}} dw = \frac{\Gamma(k_W, \frac{\rho_{Th2}}{\theta_W})}{\Gamma(k_W)} \tag{16}$$

where $W \triangleq \sum_{i=1}^{N} \tau_i |h_{2i}|^2 and\ W \sim Gamma(k_W, \theta_W)$.

Consequently, the final probability is expressed in the form of relation (17). To compute this probability, the following new variables are defined: $\mu_i \triangleq (a_{2i} - \gamma_{Th2} a_{1i})$, and $\rho_{Th2} \triangleq \frac{\gamma_{Th2}}{\gamma_0}$.

$$P_3 = P\{\gamma_2 + \gamma_c \geq \gamma_{Th2}\} = \tag{17}$$
$$P\left\{\frac{\gamma_0(\sum_{i=1}^{N} a_{2i}|h_{2i}|^2 + \sum_{i=1}^{N}|h_{3i}|^2)}{\gamma_0 \sum_{i=1}^{N} a_{1i}|h_{2i}|^2 + 1} \geq \gamma_{Th2}\right\} = P\left\{\sum_{i=1}^{N} \mu_i |h_{2i}|^2 + \sum_{i=1}^{N} |h_{3i}|^2 \geq \rho_{Th2}\right\}$$

Since the channel fading coefficients follow a Rayleigh statistical distribution, the variables $|h_{2i}|^2$ and $|h_{3i}|^2$ in (17) are modeled as independent exponential random variables for the *i-th* sub-channel. Their weighted sums are then approximated by Gamma distributions, similar to (13) and

(16), leading to the approximation in (20), where $U \triangleq \sum_{i=1}^{N} \mu_i \, |h_{2i}|^2$ and $V \triangleq \sum_{i=1}^{N} |h_{3i}|^2$, with the corresponding Gamma distributions as follows:

$$|h_{2i}|^2 \sim Exp(\lambda_{2i}) \overset{\Sigma}{\Rightarrow} U \sim Gamma(k_U, \theta_U) \tag{18}$$

$$|h_{3i}|^2 \sim Exp(\lambda_{3i}) \overset{\Sigma}{\Rightarrow} V \sim Gamma(k_V, \theta_V) \tag{19}$$

Hence, equation (17) is rewritten as follows:

$$P_3 = P\{\gamma_2 + \gamma_c \geq \gamma_{Th2}\} = P\{U + V \geq \rho_{Th2}\} \tag{20}$$

Given that the two variables U and V follow Gamma distributions and are statistically independent $(U \perp V)$, their linear combination $T = U + V$ can be approximated by another Gamma-distributed variable, i.e., $T \sim Gamma(k_T . \theta_T)$. herefore, the probability P_3 is calculated as follows [21]:

$$P_3 = P\{U + V \geq \rho_{Th2}\} = P\{T \geq \rho_{Th2}\} = F_T(\rho_{Th2}) = \tag{21}$$

$$\int_{\rho_{Th2}}^{\infty} f_T(t)dt = \int_{\rho_{Th2}}^{\infty} \frac{1}{\Gamma(k_T)\theta_T^{k_T}} t^{k_T - 1} e^{-\frac{t}{\theta_T}} dt = \frac{\Gamma(k_T, \frac{\rho_{Th2}}{\theta_T})}{\Gamma(k_T)}$$

Based on equations (13), (14), (16), and (21), the connectivity probability of the cell-edge user in the CNOMA-based system can be determined by systematically combining the derived expressions. Specifically, by substituting these results into the analytical framework, the overall connectivity probability is calculated as shown in equation (22) below.

$$CP_{MIMO\_CNOMA} = P\{\gamma_{tot2} \geq \gamma_{Th2}\} = P_1 P_2 + \bar{P}_1 P_3 = \frac{\gamma\left(k_Z, \frac{\rho_{Th1}}{\theta_Z}\right)}{\Gamma(k_Z)} \frac{\Gamma\left(k_W, \frac{\rho_{Th2}}{\theta_W}\right)}{\Gamma(k_W)} + \frac{\Gamma\left(k_Z, \frac{\rho_{Th1}}{\theta_Z}\right)}{\Gamma(k_Z)} \frac{\Gamma\left(k_T, \frac{\rho_{Th2}}{\theta_T}\right)}{\Gamma(k_T)} = \tag{22}$$

$$\frac{\gamma\left(k_Z, \frac{\rho_{Th1}}{\theta_Z}\right)\Gamma\left(k_W, \frac{\rho_{Th2}}{\theta_W}\right)}{\Gamma(k_Z)\Gamma(k_W)} + \frac{\Gamma\left(k_Z, \frac{\rho_{Th1}}{\theta_Z}\right)\Gamma\left(k_T, \frac{\rho_{Th2}}{\theta_T}\right)}{\Gamma(k_Z)\Gamma(k_T)}$$

In the next section, the performance of the derived closed-form expression for the connectivity probability of U2 in the CNOMA-based system is evaluated through computer simulations.

V. SIMULATION RESULTS

In this section, we evaluate the closed-form expression for the connectivity probability (CP) of user U2 in a CNOMA-based MIMO cellular system through computer simulations conducted in MATLAB. To validate the analytical CP, we employ the **Monte Carlo method**, a statistical simulation technique used to assess wireless system performance under random channel conditions, such as Rayleigh fading or correlated MIMO channels. The simulations generate numerous independent realizations of channel coefficients and user-specific parameters to compute the SINR and corresponding connectivity outcomes for cell-edge users. By aggregating

results over 100,000 iterations, this approach provides accurate estimates of the connectivity probability, capturing nonlinear SINR effects and coupled interference that are analytically intractable, thereby validating the derived closed-form expressions under realistic fading and power allocation scenarios. This approach follows the methodology proposed in [22] for accurate evaluation of connectivity probability in cooperative MIMO networks under stochastic channel conditions.

We then benchmark the CP performance of the CNOMA-based MIMO cellular system from the perspective of cell-edge user (U2) against three additional scenarios: (I) conventional NOMA without user cooperation, (II) a SISO system, and (III) the connectivity probability of the near user (U1) reported for reference under the same system settings. In all simulations, a circular cell of radius 100 m with a single base station located at the cell center is considered. The relay position is drawn

uniformly at random within 2–50 m from the base station, while the cell-edge user is placed uniformly at random within 80–100m from the base station. Owing to the variety of scenarios assessed, the remaining simulation parameters used in each experiment are specified precisely in the caption of the corresponding figure.

Fig. 2 compares the obtained results for $CP_{MIMO\ CNOMA}$ with the numerical outcomes of the Monte Carlo method for various values of the average SNR, i.e., the ratio of the BS total transmit power to noise power ($\gamma_0 = \frac{P_T}{N_0}$), under two distinct power allocation strategies in the MIMO CNOMA model. For a more comprehensive evaluation, the comparison is conducted for two different power division cases: $Case\ 1: A_1 = [0.1, 0.2, 0.3], Case\ 2: A_1 = [0.05, 0.15, 0.25]$ with $A_2 = 1 - A_1$ in both cases.

The plots in Fig. 2 show that the derived closed-form CP expression for user U2 in the CNOMA-based MIMO cellular system matches closely with the Monte Carlo simulation results for all considered values of γ_0 and for both power allocation cases with N = 3 transmit antennas. Moreover, Fig. 2 illustrates that, for the same total transmit power, the CP of U2 is lower in Case 1 compared to Case 2. This is because, in Case 1, the signal to interference plus noise ratio (SINR) of the direct BS–U2 link is reduced. In addition, the SINR of U1 for decoding the U2 message is also lower, thereby reducing the likelihood of cooperative forwarding. As an example, a close-up view of the results around $\gamma_0 \cong 7\ dB$ reveals that the CP of the cell-edge user in Case 2 is approximately 103.85% higher than in Case 1.

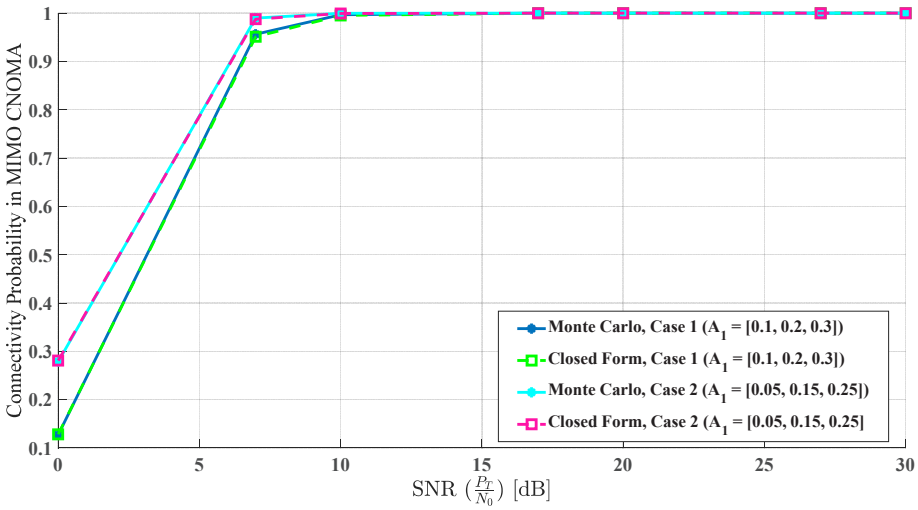

Fig. 2. The connectivity of the cell-edge user (U_2) for different average SNR values ($\sigma_1^2 = \sigma_3^2 = 0dB, \sigma_2^2 = -3dB, \gamma_{Th1} = \gamma_{Th2} = 2$) with different power allocations and $N = 3$ MIMO ($Case\ 1$: $A_1 = [0.1, 0.2, 0.3]$, $Case\ 2$: $A_1 = [0.05, 0.15, 0.25]$)

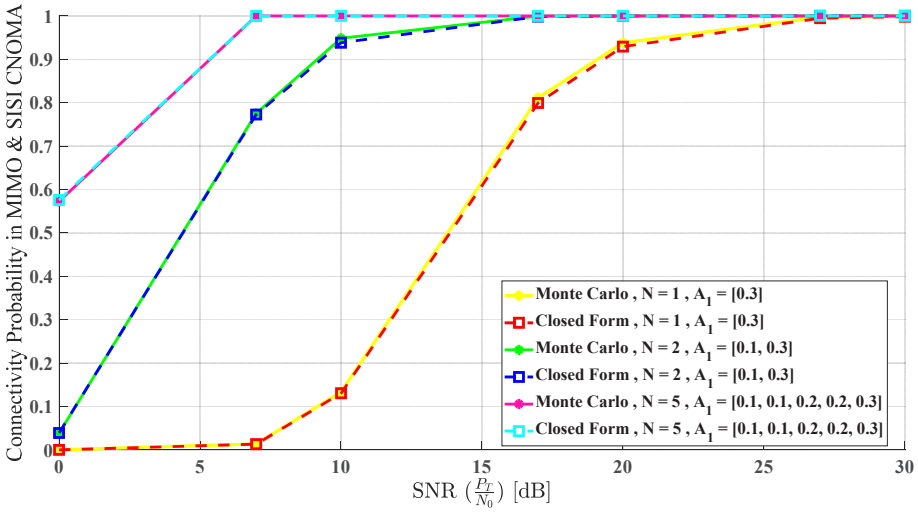

Fig. 3. The connectivity of the cell-edge user (U_2) for different average SNR values ($\sigma_1^2 = \sigma_3^2 = 0dB, \sigma_2^2 = -3dB, \gamma_{Th1} = \gamma_{Th2} = 2$) with different power allocations and N = [1, 2, 5] MIMO & SISO ($A_1 = [0.3], [0.1, 0.3], [0.1, 0.1, 0.2, 0.2, 0.3]$)

Fig. 3 investigates the effect of the number of transmit antennas (or sub-channels) on the CP performance under a fixed power allocation strategy. As expected, increasing N enhances the CP of user U2 due to the additional spatial diversity gain provided by MIMO transmission. For comparison, in our previous work [8], which considered a single-antenna (SISO) system with N = 1, the CP was significantly lower than in the current study based on MIMO systems. For instance, at $\gamma_0 \cong 7\ dB$, increasing the number of antennas from N = 1 (SISO) to N = 2 (MIMO) improves the CP by approximately 5850.46%, representing a substantial relative gain. Further increasing N from 2 to 5 also raises the CP by an additional 129.38%. The analytical and numerical simulation

results remain in excellent agreement, with deviations consistently below 1%.

Fig. 4 illustrates the CP performance for both the near user (U1) and the cell-edge user (U2) for different numbers of transmit antennas N = [1, 2, 5], comparing two systems based on MIMO and SISO under a specific NOMA condition (without near user cooperation). It can be observed that at $\gamma_0 = 10\ dB$, the CP of U1 for N = [2, 5] improves by approximately 131.17% and 164.14%, respectively, compared to the single antenna case, and this advantage is maintained across the entire SNR range due to its shorter distance to the BS and more favorable channel conditions. A similar increasing trend in CP improvement with the number of antennas is also evident for the cell-edge user (U2), where at the same SNR, the use of 2 and 5 antennas results in CP improvements of 3430.73% and 5189.06%, respectively, compared to the single-antenna model.

This performance enhancement can be attributed to two key factors: (I) for U1, the relatively short BS user distance leads to inherently high SINR even in SISO mode, while the introduction of additional transmit antennas provides spatial diversity gain and array gain, thereby further reducing the probability of SINR falling below the target threshold; and (II) for U2, which experiences significantly worse channel conditions and higher path loss due to its location at the cell edge, the increase in N offers substantial spatial diversity benefits in Rayleigh fading environments, effectively mitigating deep fading events and greatly boosting the reliability of the direct BS–U2 link. Consequently, the relative CP improvement for U2 is markedly higher than that of U1, since MIMO transforms a weak and unreliable link into a highly reliable one.

Fig. 5 presents a comparison between the analytical results derived for $CP_{MIMO\ CNOMA}$ and Monte Carlo simulation outcomes for various cooperation threshold levels γ_{Th1}, power allocation ratios $A_1 = [0.1]$ and $A_1 = [0.1, 0.15]$, under two different numbers of transmit antennas N = [1, 2] and SNR values [7, 10] dB. The results show that increasing γ_{Th1} leads to a reduction in the connection probability (CP) of U2, since the likelihood of cooperation from U1 decreases. On the other hand, when γ_{Th1} is set to a very small value, the relay user still transmits a cooperative signal even when the direct link to the cell-edge user provides satisfactory quality. This behavior results in a significant energy waste for the relay user. Moreover, transmitting the cooperative signal when the relay has decoded a weak signal from the cell-edge user after performing SIC can increase the error probability at U2. Therefore, while lowering γ_{Th1} improves CP, this improvement comes at the cost of increased relay energy consumption and a higher error probability at the cell-edge user. This trade-off between system performance and energy efficiency highlights the necessity of developing intelligent algorithms for dynamically adjusting γ_{Th1} so that the threshold can automatically adapt to varying channel conditions and user requirements.

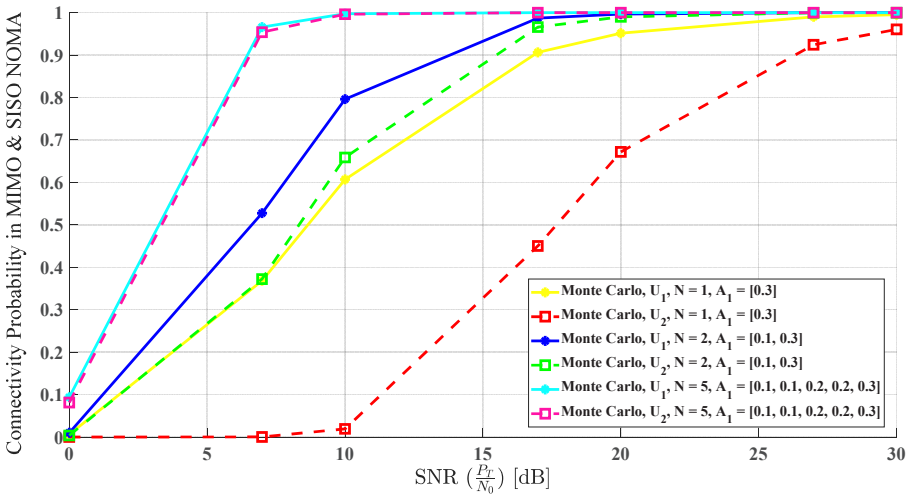

Fig. 4. The connectivity of near user (U_1) and cell-edge user (U_2) for different average SNR values ($\sigma_1^2 = 0dB, \sigma_2^2 = -3dB, \gamma_{Th1} = 1.5, \gamma_{Th2} = 2$) with different power allocations and $N = [1, 2, 5]$ MIMO & SISO ($A_1 = [0.3], [0.1, 0.3], [0.1, 0.1, 0.2, 0.2, 0.3]$)

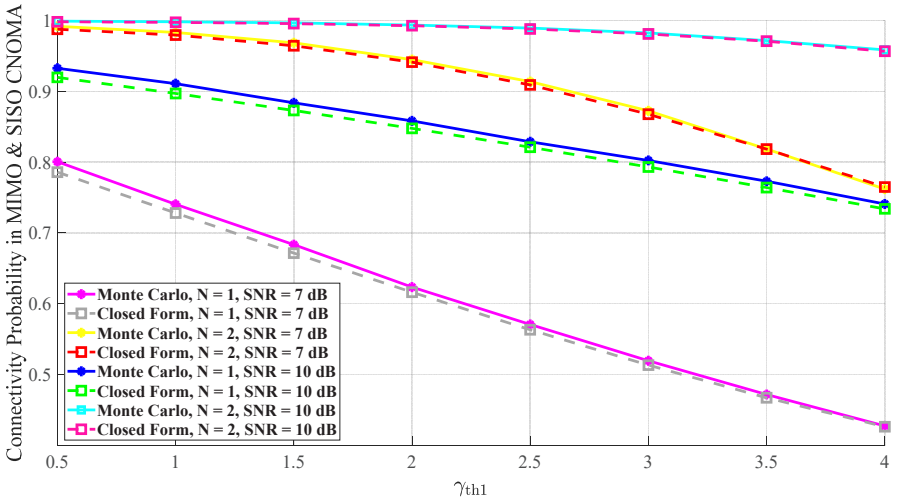

Fig. 5. The connectivityof the cell-edge user (U_2) for different threshold values ($\gamma_0 = [7, 10]\ dB, \sigma_1^2 = \sigma_3^2 = 0dB,\ \sigma_2^2 = -3dB, \gamma_{Th2} = 2$) with different power allocations and $N = [1, 2]$ MIMO & SISO ($A_1 = [0.1], [0.1, 0.15]$)

An important observation in Fig. 5 is that the difference in CP between the two power allocation schemes $A_1 = [0.1]$ and $A_1 = [0.1, 0.15]$ increases with higher γ_{Th1} values. This indicates the significant role of U1's cooperation in maintaining the connection for the cell-edge user when the direct link power is low. For instance, in a portion of the plots with $\gamma_{Th1} = 2.5\ dB$, the CP of the cell-edge user in the MIMO CNOMA case with $A_1 = [0.1, 0.15]$ and N = 2 is approximately 161.47% higher than in the SISO CNOMA case with $A_1 = [0.1]$ and N = 1 [8]. When γ_{Th1} increases to 4, this difference rises to about 179.54%. This clearly demonstrates the substantial performance gain of the proposed MIMO-based framework over the previous SISO system.

Overall, the simulation results not only validate the proposed closed-form expressions with an average analytical simulation error of less than 1%, but also provide a comprehensive comparison of system performance across CNOMA and conventional NOMA, as well as SISO [8] and MIMO configurations. These results highlight the trade-offs between power allocation, number of transmit antennas, and cooperation thresholds, clearly demonstrating the significant benefits of employing multiple antennas in MIMO systems for improved connectivity and reliability compared to the SISO scenario in our previous work [8].

VI. CONCLUSION

This paper presented a comprehensive statistical analysis of the connectivity probability for cell-edge users (U2) in MIMO-based cooperative non-orthogonal multiple access (CNOMA) wireless cellular networks. In the proposed framework, intra-cell users can act as relays to alleviate connectivity limitations for cell-edge users. A closed-form analytical expression for the connectivity probability of U2 was derived by employing vectorized power allocation, subchannel specific SINR modeling under Rayleigh fading, and a Gamma distribution and weighted exponential sums approximation. The model incorporates the impact of imperfect successive interference cancellation (SIC) at the relay, accounts for the fading characteristics of the involved channels, and quantifies the positive role of user cooperation in improving connectivity.

Furthermore, an extensive comparative study was conducted between conventional NOMA and the proposed CNOMA scheme. Simulation results demonstrated that MIMO CNOMA significantly outperforms conventional NOMA and the previous SISO-based work [8], particularly in reducing the outage probability of cell-edge users, especially in severe fading environments. This performance gain stems from inter-user cooperation, resource sharing, and power allocation diversity, which enable the system to more effectively maintain connectivity under harsh channel conditions. For example, based on the combined analysis of Figs. 3 and 4, when the direct link power is severely attenuated and $\gamma_0 = 7dB$, the outage probability in $\text{MIMO}_{\text{N}}=5$ CNOMA is up to 3027.79 times lower than that of conventional SISO CNOMA [8]. These results underscore the strong potential of MIMO CNOMA for enhancing link reliability in challenging propagation environments.

Importantly, the proposed framework provides several distinct advantages over the prior SISO study [8]. The Spatial Diversity Gain inherent in MIMO systems enhances reliability, while the Generality of the Framework allows evaluation across various antenna configurations from SISO to massive MIMO. The Power Allocation Flexibility enables optimized distribution of power across sub-channels, and the methodology, including Gamma Distribution and Weighted

Exponential Sums, allows precise closed-form performance evaluation. Moreover, the study is Closer to Practical Scenarios, reflecting realistic multi-antenna wireless networks such as 5G/6G and Wi-Fi 6/7.

Nevertheless, CNOMA's performance improvements come with design challenges. The cooperation threshold γ_{Th1} plays a critical role in balancing system performance and energy consumption. Reducing γ_{Th1} increases connectivity probability but also raises the relay's energy usage and the error probability at the cell-edge user. Conversely, increasing γ_{Th1} reduces cooperation probability and increases the risk of outage. This trade-off highlights the necessity of developing intelligent algorithms for dynamic threshold adjustment, enabling real-time adaptation to varying channel conditions and user requirements.

In conclusion, the results of this study confirm that MIMO CNOMA is a promising and effective solution for improving communications in severely faded environments, particularly for cell-edge users, and clearly surpasses the capabilities of previous SISO-based approaches [8]. Achieving optimal performance requires careful design of system parameters such as power allocation, cooperation thresholds, and the consideration of imperfect channel state information, user mobility, and advanced cooperative strategies, including full-duplex relaying and reconfigurable intelligent surfaces (RIS). These findings can serve as a foundation for future research aimed at optimizing MIMO CNOMA systems and developing intelligent resource management algorithms for next-generation wireless networks.

REFERENCES

[1] J. Sheeba, V. B. Kumaravelu and A. L. Imoize,"Rate Maximization of Cell-Edge Users Through Cooperative Non-Orthogonal Multiple Access," in *Proceedings 4th International Conference on Signal Processing and Communication (ICSPC)*, " Coimbatore, India, Mar. 23–24, 2023, pp. 361-366.

[2] T. T. Nguyen, S. Q. Nguyen, P. X. Nguyen and Y. H. Kim, "Evaluation of Full-Duplex SWIPT cooperative NOMA-Based IoT relay networks over Nakagami-m fading channels," *Sensors,* vol. 22, no. 5, p. 1974, May 2022.

[3] Y. Wang, L. Xiang, J. Zhang and X. Ge, "Connectivity Analysis for Large-Scale Intelligent Reflecting Surface Aided mm Wave Cellular Networks.," in *Proceedings IEEE 33rd Annual International Symposium on Personal, Indoor and Mobile Radio Communications (PIMRC)*, Kyoto, Japan, Sep. 2022, pp. 1-6.

[4] T. N. Do, D. B. da Costa, T. B. Duong and B. An, "Improving the performance of cell-edge users in NOMA systems using cooperative relaying," *IEEE Trans. Communications,* vol. 66, no. 5, pp. 1883-1901, May 2018.

[5] S. Zeng, X. Huang and D. Li, "Joint Communication and Computation Cooperation in Wireless Powered Mobile Edge Computing Networks with NOMA," *IEEE Internet of Things Journal,* vol. 10, no. 11, pp. 9849 - 9862, Nov. 2023.

[6] A. A. Saleh and M. A. Ahmed, "Performance enhancement of cooperative MIMO-NOMA systems over sub-6 GHz and mmWave bands," *Journal of Telecommunications and Information Technology*, vol. 92, no. 2, pp. 70–77, Jun. 2023

[7] A. A. Amin and S. Y. Shin, "Capacity analysis of cooperative NOMA-OAM-MIMO based full-duplex relaying for 6G," *IEEE Wireless Communications Letters*, vol. 10, no. 7, pp. 1395–1399, Jul. 2021

[8] A. Bagheri and M. A. Karimi, "The Impact of Using the Non-Orthogonal Multiple Access Technique in Collaborative Wireless Cellular Networks on Improving Communication Quality," *Journal of Soft Computing and Information Technology*, vol. 14, no. 1, pp. 37–44, Jun. 2025.

[9] O. Alamu, T. O. Olwal and K. Djouani, "Cooperative NOMA networks with simultaneous wireless information and power transfer: An overview and outlook," *Alexandria Engineering Journal,* vol. 71, pp. 413-438., Apr. 2023.

[10] T. Do, D. da Costa, T. Duong and B. An, "Improving the performance of cell-edge users in MISO-NOMA systems using TAS and SWIPT-based cooperative transmissions," *IEEE Trans. Green Communications and Networking,* vol. 2, no. 1, pp. 49-62, Mar. 2017.

[11] N. Zaman, A. Hassan, Z. Abbas, G. Abbas, M. Bilal and S. Pack, "Performance analysis of NOMA enabled multi-user co-operative IoT network with SWIPT protocol," *Journal of King Saud University-Computer and Information Sciences,* vol. 38, no. 5, p. 1016, Jul. 2023.

[12] X. Xing, J. Cao and H. Zhou, "Improving Quality of Service for Cell-Edge Users in D2D-Relay Networks," *Wireless Personal Communications,* vol. 126, no. 2, pp. 1789-1804, Jun. 2022.

[13] C. Le, D. Do and M. Voznak, "Wireless-powered cooperative MIMO NOMA networks: Design and performance improvement for cell-edge users," *Electronics,* vol. 8, no. 3, p. 328, Mar. 2019.

[14] M. Shirazi and M. Zahabi, "A novel full-duplex relay selection and resource management in cooperative SWIPT NOMA networks," *Journal of Electrical and Computer Engineering Innovations (JECEI),* vol. 11, no. 1, pp. 161-172, Jan. 2023.

[15] F. Kara and H. Kaya, "Threshold-based selective cooperative-NOMA," *IEEE Communications Letters,* vol. 23, no. 7, pp. 1263-1266, Jul. 2019.

[16] M. M. da Silva and R. Dinis, "Power-Ordered NOMA with Massive MIMO for5 G Systems," *Journal of Applied Sciences,* vol. 11, no. 8, article 3541, Apr. 2021.

[17] M. W. Xie, X. Ding, B. Cai, X. Li and M. Wei, "Downlink MIMO-NOMA System for6 G Internet of Things," *Journal of Electronics,* vol. 11, no. 19, article 3233, Oct. 2022.

[18] M. Ghous, A. K. Hassan, Z. H. Abbas, G. Abbas, A. Hussien, and T. Baker, " Cooperative Power-Domain NOMA Systems: An Overview," *Journal of Sensors,* vol. 22, no. 24, article 9652, Dec. 2022.

[19] M. Hassan, M. S. Goraya, K. Hamid, R. Saeed, M. Abdelhaq, and R. Alsaqour, " Design of Power Location Coefficient System for 6G Downlink Cooperative NOMA Network," *Journal of Energies,* vol. 15, no. 19, article 6996, Sep. 2022.

[20] M. Fadhil, N. F. Abdullah, M. Ismail, R. Nordin, A. Saif, and M. Al-Obaidi, " Power Allocation in Cooperative NOMA MU-MIMO Beamforming Based on Maximal SLR Precoding for 5G," *Journal of Communications,* vol. 14, no. 8, pp. 676–683, Aug. 2019.

[21] A. Papoulis and P. Unnikrishna, *Probability, random variables and stochastic process*, 4th Edition, Boston, USA: McGraw-Hill, 2002, ch. 4-7, pp. 72-303.

[22] S. M. Ross, *Introduction to Probability and Statistics for Engineers and Scientists*, 6th Edition, San Diego, CA, USA: Academic Press, 2020, ch. 5 & 15, pp. 151-221 & 619-649.